March 2004

Phys. Chem. News 16 (2004) 46-53 PCN

BAND-STRUCTURE AND TRANSPORT CALCULATIONS IN QUANTUM WIRES USING A TRANSFER-MATRIX TECHNIQUE

A. Mayer

Laboratoire de Physique du Solide,
Faculté Universitaires Notre-Dame de la Paix,
Rue de Bruxelles 61, B-5000 Namur, Belgium
** Corresponding author. E-mail : alexandre.mayer@fundp.ac.be*
Received : 15 February 2003 ; revised version accepted :29 June 2003

Abstract

The transfer-matrix methodology is used to solve linear systems of differential equations, in situations where the solutions of interest are in the continuous part of the energy spectrum. The technique is actually a generalization in three dimensions of methods used to obtain scattering solutions in one dimension. Using the layer-addition algorithm allows one to control the stability of the computation and describe efficiently periodic repetitions of a basic unit. The paper provides a pedagogical presentation of this technique. It also describes in details how the band structure associated with an infinite periodic medium can be extracted from the transfer matrices characterizing a single basic unit. The method is applied to the calculation of the transmission and band structure of electrons subject to cosine potentials in a cylindrical wire. The simulations show that bound states must be considered because of their impact as sharp resonances in the transmission diagram and to obtain complete band structures. Additional states only improve the completeness of the representation.

Keywords: Electronic Scattering; Transfer Matrix; Band Structure; Bound States.

1. Introduction

The transfer-matrix methodology is one of the techniques used to solve linear systems of differential equations, in situations where the solutions of interest are in the continuous part of the energy spectrum. For this numerical scheme to be relevant, the physical system considered should be located between two separate boundaries (standing for the regions of incidence and transmission). Given a set of basis states used for the expansion of the wave function, the transfer matrices provide, for each state incident on one boundary of the system, the coefficients of the corresponding reflected and transmitted states.

The advantage of this technique is that it does not require the storage of the wave function in the intermediate part of the system (where solutions are only propagated through). Its storage space requirements therefore depend essentially on the number N of basis states used for the expansion of the solutions (more precisely on N^3), and not directly on the dimensions of the system. This technique was first developed by Pendry [1-4] for Low Energy Electron Diffraction simulations. It was used and developed by other authors [5-15], including Mayer et al. [16-18] for the simulation of the Fresnel projection microscope [19-22] and for the modeling of (photon-stimulated) field emission [23-24].

An interesting feature of the method is that it can easily handle periodic repetitions of a basic unit. From the transfer matrices associated with a single unit of the structure, it is indeed straightforward (using the layer-addition algorithm [1-2]) to derive those corresponding to an arbitrary number of units. The band structure that characterizes the infinite repetition of these units can also be extracted from the transfer matrices.

It is the objective of this paper to provide a pedagogical presentation of the transfer-matrix methodology and describe how band structures can be derived in this approach. The theoretical aspects of this scheme are developed in Sec. II. The technique is then applied in Sec. III to the study of electrons that are confined in a cylindrical wire and subject to cosine potentials. The simulations show how fast band structure effects appear with the number of periods. The features of the transmission diagram are related to those of the band structure and interpreted in terms of quantum conductance and band-gap effects. The issue of bound states is also considered. It is found that they need to be considered in order to reproduce sharp resonances in the transmission diagram and to obtain complete band structures. Additional states only improve the completeness of the representation.

2. Theory

Let us consider three regions: the Region I ($z \leq 0$), the Region II ($0 \leq z \leq D$) and the Region III ($z \geq D$). We consider the scattering strengths to be

in the intermediate Region II and want to compute how electronic states incident on one side of the Region II are scattered towards the other.
Let us consider two sets of basis states in the two boundary Regions I and III, namely $\{\Psi_j^{I,\pm}\}$ and $\{\Psi_j^{III,\pm}\}$. These states are used to expand the wave function in the Regions I and III, for a given value of the energy E. The subscript j enumerates the allowed values of $\{k_\rho,m\}$ in cylindrical coordinates ($\{k_x,k_y\}$ in cartesian coordinates), considering boundary conditions and the energy E. The ± signs refer to the propagation direction relative to the z axis, which is oriented from the Region I to the Region III (see Fig. 1).

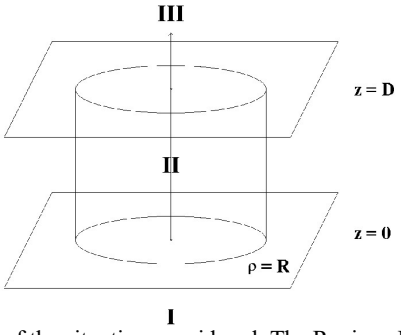

Figure 1 : Schematic representation of the situation considered. The Regions I and III are the regions of incidence and transmission. The intermediate Region II contains a cylindrical wire with cosine potentials.

We assume that these states are separable in the following way:

$$\Psi_j^{I,\pm}(\rho,\phi,z) = \psi_j(\rho,\phi)\exp(\pm ik_{z,j}z)\,, \tag{1}$$

$$\Psi_j^{III,\pm}(\rho,\phi,z) = \psi_j(\rho,\phi)\exp(\pm ik_{z,j}z)\,. \tag{2}$$

These relations will be used to derive band structures and are only required for this specific application.
We will describe in this section how scattering solutions, corresponding to a single incident state $\Psi_j^{I,+}$ in the Region I or $\Psi_j^{III,-}$ in the Region III can be derived. We will describe shortly the layer-addition algorithm and finally explain how the band structure associated with the infinite repetition of a basic unit can be extracted from these solutions.

2.1 Basic formulation of the transfer-matrix technique

The first step of the technique consists in establishing solutions associated with single outgoing $\Psi_j^{III,+}$ or incoming $\Psi_j^{III,-}$ states in the Region III. Since the wave function and its derivatives are entirely defined in the Region III, one can propagate these states numerically from $z=D$ to $z=0$, where the solutions are expanded in terms of incident $\Psi_j^{I,+}$ and reflected $\Psi_j^{I,-}$ states. The corresponding expansion coefficients are stored in $\mathbf{T}^{\pm\pm}$ matrices and we end up with the following set of solutions:

$$\overline{\Psi}_j^{+} \overset{z\le 0}{=} \sum_i T_{i,j}^{++}\Psi_i^{I,+} + \sum_i T_{i,j}^{-+}\Psi_i^{I,-} \overset{z\ge D}{=} \Psi_j^{III,+}\,, \tag{3}$$

$$\overline{\Psi}_j^{-} \overset{z\le 0}{=} \sum_i T_{i,j}^{+-}\Psi_i^{I,+} + \sum_i T_{i,j}^{--}\Psi_i^{I,-} \overset{z\ge D}{=} \Psi_j^{III,-}\,. \tag{4}$$

In the second step of the procedure, these solutions are combined linearly in order to derive new solutions satisfying the scattering boundary conditions, namely solutions associated with either a single incident state $\Psi_j^{I,+}$ in the Region I or a single incident state $\Psi_j^{III,-}$ in the Region III (with this time reflected states in the region of incidence and transmitted states in the other one). Formally, these solutions are expressed in terms of $\mathbf{S}^{\pm\pm}$ matrices in the following way:

$$\Psi_j^{+} \overset{z\le 0}{=} \Psi_j^{I,+} + \sum_i S_{i,j}^{-+}\Psi_i^{I,-} \overset{z\ge D}{=} \sum_i S_{i,j}^{++}\Psi_i^{III,+}\,, \tag{5}$$

$$\Psi_j^{-} \overset{z\le 0}{=} \sum_i S_{i,j}^{--}\Psi_i^{I,-} \overset{z\ge D}{=} \Psi_j^{III,-} + \sum_i S_{i,j}^{+-}\Psi_i^{III,+}\,. \tag{6}$$

The $\mathbf{S}^{\pm\pm}$ matrices, which contain the expansion coefficients of these solutions are related to the $\mathbf{T}^{\pm\pm}$ matrices of Eqs 3 and 4 by $\mathbf{S}^{++}=(\mathbf{T}^{++})^{-1}$, $\mathbf{S}^{-+}=\mathbf{T}^{-+}(\mathbf{T}^{++})^{-1}$, $\mathbf{S}^{--}=\mathbf{T}^{--}-\mathbf{T}^{-+}(\mathbf{T}^{++})^{-1}\mathbf{T}^{+-}$ and $\mathbf{S}^{+-}=-(\mathbf{T}^{++})^{-1}\,\mathbf{T}^{+-}$.

2.2 The layer-addition algorithm for the control of accuracy and the description of periodic systems

To control the numerical instabilities that appear with large distances D (when inverting $\mathbf{T}^{++}$ to obtain the $\mathbf{S}^{\pm\pm}$ matrices) or to treat efficiently periodic systems, it is useful to use the layer-addition algorithm [1-2]. Given a subdivision $0=z_0<z_1<z_2<\ldots<z_{n-1}<z_n=D$ of the interval $[0,D]$ and referring by $S^{++}_{z_i,z_j}$, $S^{-+}_{z_i,z_j}$, $S^{--}_{z_i,z_j}$ and $S^{+-}_{z_i,z_j}$ to the S matrices associated with the interval $[z_i,z_j]$, one can derive those associated with the entire interval $[0,D]$ from the recursive application of the following relations:

$$S^{++}_{z_0,z_i} = S^{++}_{z_{i-1},z_i}\left[I - S^{+-}_{z_0,z_{i-1}} S^{-+}_{z_{i-1},z_i}\right]^{-1} S^{++}_{z_0,z_{i-1}}, \quad (7)$$

$$S^{--}_{z_0,z_i} = S^{--}_{z_0,z_{i-1}}\left[I - S^{-+}_{z_{i-1},z_i} S^{+-}_{z_0,z_{i-1}}\right]^{-1} S^{--}_{z_{i-1},z_i}, \quad (8)$$

$$\begin{aligned} S^{-+}_{z_0,z_i} &= S^{-+}_{z_0,z_{i-1}} + S^{--}_{z_0,z_{i-1}} S^{-+}_{z_{i-1},z_i} \\ &\times\left[I - S^{+-}_{z_0,z_{i-1}} S^{-+}_{z_{i-1},z_i}\right]^{-1} S^{++}_{z_0,z_{i-1}} \end{aligned}, \quad (9)$$

$$\begin{aligned} S^{+-}_{z_0,z_i} &= S^{+-}_{z_{i-1},z_i} + S^{++}_{z_{i-1},z_i} S^{+-}_{z_0,z_{i-1}} \\ &\times\left[I - S^{-+}_{z_{i-1},z_i} S^{+-}_{z_0,z_{i-1}}\right]^{-1} S^{--}_{z_{i-1},z_i} \end{aligned}. \quad (10)$$

These relations enable a straightforward derivation of the S matrices associated with the periodic repetition of an arbitrarily large number of units once the transmission through a single unit has been established. Even in the case of non-periodic systems, it is generally useful to use this algorithm since the relative error on the transfer-matrix calculations increases exponentially with the distance D if it is considered in a single step. The number of subdivisions to consider in order to achieve a given accuracy is given, with other considerations on the stability of transfer-matrix calculations, in Ref. [16].

For the derivation of band structures in the next subsection, we will use the T matrices. These matrices keep stable when considering large distances D (only the inversion of $\mathbf{T}^{++}$ is unstable when D is too large). When these matrices are obtained for subdivisions of the $[0,D]$ interval, they can be updated according to the following formula:

$$\begin{aligned} \begin{pmatrix} T^{++}_{z_0,z_i} & T^{+-}_{z_0,z_i} \\ T^{-+}_{z_0,z_i} & T^{--}_{z_0,z_i} \end{pmatrix} &= \begin{pmatrix} T^{++}_{z_0,z_{i-1}} & T^{+-}_{z_0,z_{i-1}} \\ T^{-+}_{z_0,z_{i-1}} & T^{--}_{z_0,z_{i-1}} \end{pmatrix} \\ &\times \begin{pmatrix} T^{++}_{z_{i-1},z_i} & T^{+-}_{z_{i-1},z_i} \\ T^{-+}_{z_{i-1},z_i} & T^{--}_{z_{i-1},z_i} \end{pmatrix} \end{aligned}. \quad (11)$$

2.3 Derivation of band structures from transfer matrices

Let us now consider a basic unit, of length a in the z direction. One can compute the transfer matrices associated with this structure, for given values of the energy E. Our objective is to extract from these matrices the band structure characterizing the infinite, periodic repetition of this unit.

For this purpose let us first reconsider the solutions of Eqs 3 and 4, which are recast in the following way:

$$\begin{aligned} \left(\overline{\Psi}^{+}_j \ldots \overline{\Psi}^{-}_j\right) &\overset{z\le 0}{=} \left(\Psi^{I,+}_j \ldots \Psi^{I,-}_j\right)\begin{pmatrix} T^{++} & T^{+-} \\ T^{-+} & T^{--} \end{pmatrix} \\ &\overset{z\ge a}{=} \left(\Psi^{III,+}_j \ldots \Psi^{III,-}_j\right) \end{aligned}. \quad (12)$$

We want to find combinations $\left(\overline{\Psi}^{+}_j \ldots \overline{\Psi}^{-}_j\right)U$ of these solutions that satisfy the relation:

$$\left(\overline{\Psi}^{+}_j \ldots \overline{\Psi}^{-}_j\right)U\,|_{z=a} = \left(\overline{\Psi}^{+}_j \ldots \overline{\Psi}^{-}_j\right)U\,|_{z=0}\ \Lambda, \quad (13)$$

with Λ a diagonal matrix containing elements of the form $\lambda=\exp(ik_z a)$. These combinations describe particular states that keep unchanged after propagation through one period of the system except for a phase factor $\exp(ik_z a)$. These states are therefore Bloch states associated with wave vectors k_z in the first Brillouin zone $[-\pi/a,\pi/a]$ of the periodic system (for the energy E considered) and the couples of points (k_z,E) will represent the band structure of the system. By considering the propagative solutions given in Eq. 12, this relation can be written as:

$$\begin{aligned} &\left(\Psi^{III,+}_j \ldots \Psi^{III,-}_j\right)|_{z=a}\ U \\ &= \left(\Psi^{I,+}_j \ldots \Psi^{I,-}_j\right)|_{z=0}\begin{pmatrix} T^{++} & T^{+-} \\ T^{-+} & T^{--} \end{pmatrix} U\Lambda \end{aligned}. \quad (14)$$

If we now remember the expressions 1 and 2 of the basis states $\Psi^{I,\pm}_j$ and $\Psi^{III,\pm}_j$, we can relate them by

$$\begin{aligned} &\left(\Psi^{I,+}_j \ldots \Psi^{I,-}_j\right)|_{z=0} \\ &= \left(\Psi^{III,+}_j \ldots \Psi^{III,-}_j\right)|_{z=a}\ diag[e^{-ik_{z,j}a},\ldots,e^{ik_{z,j}a}] \end{aligned} \quad (15)$$

where $diag[\ ]$ stands for a diagonal matrix containing the elements in brackets, so the equation 14 finally leads to:

$$U\Lambda^{-1}U^{-1} = diag[e^{-ik_{z,j}a},\ldots,e^{ik_{z,j}a}]\begin{pmatrix} T^{++} & T^{+-} \\ T^{-+} & T^{--} \end{pmatrix} \quad (16)$$

which means that the eigen values $\overline{\lambda}$ of the matrix on the right-hand side of this expression will provide the wavevectors k_z characterizing the Bloch states associated with the energy E [through $\lambda = \overline{\lambda}^{-1} = \exp(ik_z a)$]. Note that in most techniques the values of E are obtained as a function of k_z and that the restriction of k_z in the

first Brillouin zone [-π/*a*, π/*a*] of the periodic system is automatically verified.

It has to be noted that the values of $\lambda = \overline{\lambda}^{-1}$ are not always in the form $\exp(ik_z a)$, especially in situations involving tunneling processes or in band-gap regions. Many if not all of them can indeed exhibit an exponential dependence $\exp(Ka)$ and are therefore not relevant to the band structure. One distinguishes the values λ to consider for the representation of the band structure by the condition $|\lambda|=1$ (within numerical precision).

For a given problem, this technique provides a particular *representation* of the band structure, since its structure in the three-dimensional reciprocal space is projected on the k_z axis. This is a consequence of formulating the three-dimensional scattering of the wave function as the one-dimensional propagation of its components. In general this representation is appropriate in situations where a treatment by transfer matrices is relevant.

3. Application: band structure and transport properties of cylindrical wires

The applications considered in this paper will focus on the scattering of electrons subject to cosine potentials in a cylindrical wire. We will compute the transmission through a finite number of periods and compare these results with the band structure characterizing the infinite medium. We will also study the impact of bound states in the intermediate region and discuss the necessity to consider them or not.

We assume that the radius R of the wires is identical to the period a in the z direction. Using cylindrical coordinates, the boundary states we use for the representation of the wave function in the Region I and III are given by:

$$\Psi^{+,\pm}_{m,j}(\rho,\phi,z) = \frac{J_m(k_{m,j}\rho)\exp(im\phi)}{\frac{1}{R}\sqrt{2\int_0^R d\rho\rho[J_m(k_{m,j}\rho)]^2}} \cdot \times \exp(\pm i\sqrt{\tfrac{2m}{\hbar^2}E - k_{m,j}^2}\, z) \qquad (17)$$

The radial wave vectors $k_{m,j}$ characterizing these states are solutions of $J'_m(k_{m,j}R)=0$. This condition of vanishing radial derivative of the wave function on the border of the cylinder is imposed in the entire system (Region II included). It enables the wire to allow for at least one solution, namely $k_{0,0}=0$, for any value of the energy E. The way the electronic states are propagated through the Region II is explained with details in Ref. [20,21]. In order to improve the clarity of the results, only axially symmetric states will be considered.

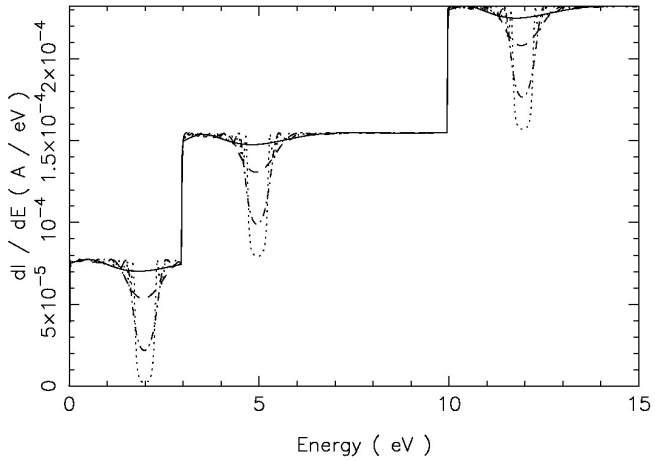

Figure 2: Values of *dI/dE* after 2 (solid), 4 (dotted), 8 (dot-dashed) and 16 (dotted) periods of a V(*z*)=0.4 cos(2π/*a z*) eV potential in a cylinder with radius *a*=0.434 nm.

3.1 Transmission and band structure for a V(*z*) = V_0 cos(2π/*a z*) potential

The first potential we consider is given by V(*z*) = V_0 cos(2π/*a z*), with V_0=0.4 eV and *a*=0.434 nm. These parameters are chosen so that a 0.4 eV-wide band gap appears at an electron energy of $\frac{\hbar^2}{2m}(\pi/a)^2$=2 eV. After calculation of the transfer matrices associated with a single period *a* of the potential and using the layer-addition algorithm presented in Sec. II.2, it is straightforward to compute how the electronic transmission in the wire changes as the number of periods increases.

We illustrated in Fig. 2 the electronic transmission (more precisely the values of *dI/dE*) for tube lengths corresponding to 2, 4, 8 and 16 periods of the potential and electron energies

ranging from 0 to 15 eV. One can observe the apparition of gaps, which tend to be more pronounced as the number of periods increases. Besides the gaps, the transmission tends to its maximal value and exhibits oscillations that are related to stationary waves in the structure. Indeed their number and the sharpness of their contribution in the transmission diagram increase with the number of periods. Similar observations were made when studying the conduction and field-emission properties of the semiconducting (10,0) carbon nanotube [25].

These non-zero values of the transmission at energies where a band-gap exists when the medium is infinite is due to the finite length of the structures considered here and to the existence of exponentially decaying solutions in these regions. It is only in truly infinite structures that these solutions are prohibited because of their exploding behavior at either z=+∞ or -∞. The existence of decaying solutions in band-gaps was invoked in Ref. [24] to justify the presence of photon-excited electrons in the gap of a (10,0) nanotube (in the context of field emission).

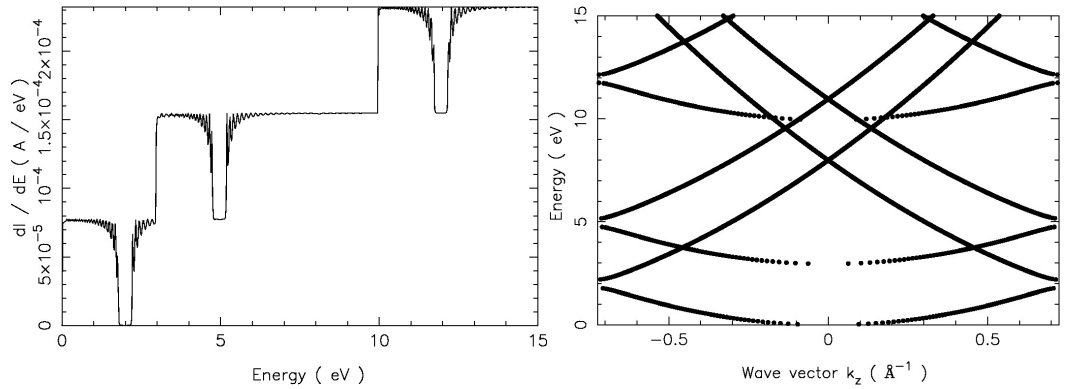

Figure 3: Left: values of *dI/dE* after 32 periods of a V(*z*)=0.4 cos(2π/*a z*) eV potential in a cylinder with radius *a*=0.434 nm. Right: band structure characterizing the infinite medium.

The values of the transmission after 32 periods of the potential and the band structure characterizing the infinite medium are represented in Fig. 3. The gaps in the transmission diagram are now well pronounced and in agreement with those in the band structure. There is a step in the transmission each time the energy is sufficient to allow for a new state in the radial direction. The occurrence of these steps coincide with the beginning of new bands in the band structure. The height of the steps is given by $2e^2/h$ (7.74×10^{-5} Ω^{-1}), which is twice the value of the conductance quantum since each basis state is representative of two electrons with opposite spins. Because of the value of the period *a*, the gaps follow always by 2 eV the steps in the transmission diagram, which reflects the fact that the band-gaps are always 2 eV higher in energy than the beginning of the new bands.

It is interesting to notice that the energy where all transitions or gaps appear are close to integer values (in eV)! In particular, the steps associated with new solutions appear at 3 and 10 eV. This peculiarity can be explained by the fact that the solutions of the boundary condition $J'_0(k_{0,j}a)=0$ are given by $k_{0,j}a = (j+1/4)\,\pi$ (in a first approximation [26]). If we remember that *a* was chosen so that $\frac{\hbar^2}{2m}(\pi/a)^2 = 2$ eV, it can easily be shown that the energy associated with the lateral wave vectors $k_{0,j}$ is given approximately by $E_{0,j}= (2j^2+j+1/8)$ eV, which explains our observations and predicts the position of the next steps.

3.2 The issue of bound states with a V(ρ)=V₀ cos(2π/*T* ρ) potential

We will now address the issue of bound states in the intermediate Region II and the related question of the number of basis states to consider in this region. In the Regions I and III, the number of basis states is fixed by the condition $\frac{\hbar^2 k_{m,j}^2}{2m} \le E$. Indeed basis states with higher $k_{m,j}$ values would be real exponentials in the *z* direction, carrying no current and causing only instabilities (we assume the potential energy to be zero in the Regions I and III). Since however the potential energy in the intermediate Region II can take negative values, the condition on $k_{m,j}$ inside the Region II must be relaxed to $\frac{\hbar^2 k_{m,j}^2}{2m} \le E + \Delta E$ and there is the possibility for this region to accommodate additional states, which are exponentially decreasing outside this region but not inside.

This raises an issue on the necessity to consider these *bound states* or not. A first technical difficulty arises from the fact the number of states

in the Region II is different from that in Regions I and III. Because of that, connecting the solutions at $z=0$ and $z=D$ involves the inversion of non-square matrices [27]. All techniques required to deal efficiently with this point were however developed in Ref. [17]. Another point is that, according to the literature and for different formulations of the transfer-matrix methodology [9-10], these bound states are likely to cause numerical instabilities. Our objective was therefore to create artificially bound states in our system and study their effect as well as the necessity to consider them or not.

Let us first consider a $V(\rho)=V_0\cos(2\pi/T\,\rho)$ potential, with V_0=1 eV. The length D and radius $R=2T$ of the cylinder are increased to 1 nm. Because of its ρ-dependence - and unlike the previous case - this potential introduces a coupling between the basis states in Region II, which is a necessary condition to observe any effect associated with bound states. Since the potential is independent of z, its effect is actually to redefine the electronic states that propagate independently in the wire from the original ones (i.e., states characterized by given values of m and j) to combinations of them and one can already understand the necessity to a have enough basis states to represent these new states correctly.

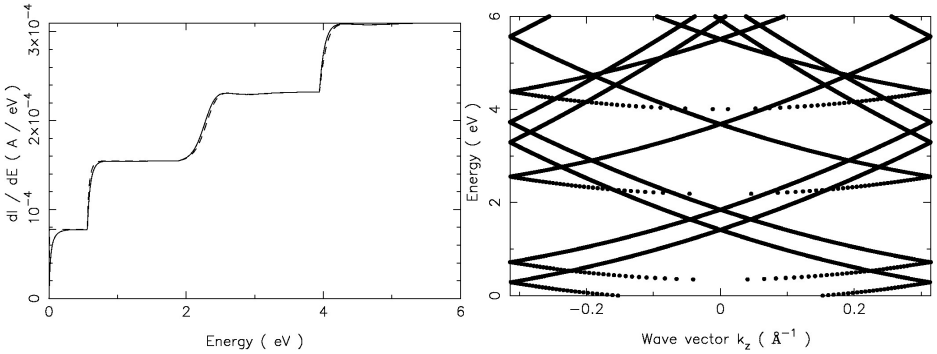

Figure 4: Left: values of dI/dE after D=1 nm of a $V(\rho)=\cos(2\pi/T\,\rho)$ eV potential in a cylinder with radius $R=2T$=1 nm. The solid curve corresponds to ΔE=20 eV and the dashed one to ΔE= 0. Right: band structure characterizing the infinite repetition of the Region II.

We represented in Fig. 4 the values of dI/dE obtained at $z=D$ as well as the band structure characterizing the infinite repetition of the Region II. These results were obtained by considering ΔE=20 eV, i.e. nine basis states within the Region II while there are only four of them in the Regions I and III. These additional states serve essentially to remove unphysical discontinuities in the band structure, which appear when the degree of completeness of the basis is poor. The role of ΔE is identical to the "cut-off energy" in plane-waves calculations and there is no effect associated with bound states, which are not present here. We checked that these results keep unchanged when considering higher values of ΔE (up to 50 eV). For the purpose of comparison we represented the values of dI/dE obtained with ΔE=0 (showing that the currents are less sensitive to the completeness of the basis than the band structures).

Let us now consider the $V(\rho)=V_0\cos(2\pi/T\,\rho)$-1 eV potential. We represented in Fig. 5 the corresponding values of dI/dE as well as the band structure that would characterize the Region II if repeated periodically. As expected, the band structure is shifted down by 1 eV. This means that the two bands that stood between 0 and 1 eV in Fig. 4 now give rise to discrete energy levels, characterizing bound states. The position of these energy levels is given by the intersection of the former bands with the limits $\pm\pi/D$ of the first Brillouin zone (namely at -0.71 and -0.28 eV), since the length D of the Region II is then an integer multiple of half the electronic wave length in the z direction. For the same reason, quasi-bound states in the continuum part of the spectrum ($E\geq 0$) will exist each time the bands of Fig. 5 meet the limits $\pm\pi/D$ of the first Brillouin zone.

Despite the fact these bound states only exist in the Region II, they have an impact on the propagative solutions in the $E\geq 0$ range. As observed in Ref. [9,13-15], this impact is essentially limited to localized resonances in the dI/dE values, at energies where the interaction between propagative states and (quasi-)bound ones is stronger. Indeed the two resonances in Fig. 5 appear at energies where bands meet the border of the first Brillouin zone for the first time (the electronic wave length in the z direction is then identical to that of the bound states, which enhances the interactions).

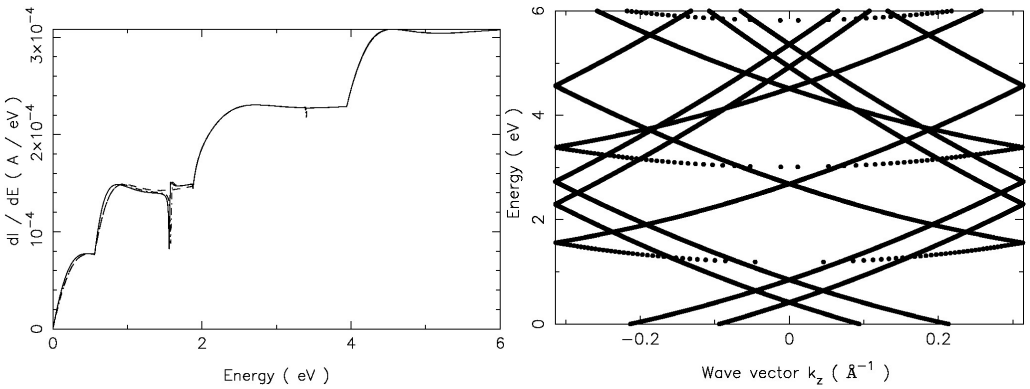

Figure 5: Left: values of *dI/dE* after *D*=1 nm of a V(ρ) = cos(2π/*T* ρ)-1 eV potential in a cylinder with radius *R*=2*T*=1 nm. The solid curve corresponds to *ΔE*=20 eV, the dashed one to *ΔE*=0 and the dot-dashed one to *ΔE*=1 eV. Right: band structure characterizing the infinite repetition of the Region II.

The results presented here were obtained by taking *ΔE*=20 eV, as required for the completeness of the basis. In particular it is necessary to consider the two bound states (which are part of the solution within the Region II). Neglecting them by taking *ΔE* =0 has indeed a strong impact on both the band structure (all bands are truncated at their beginning on the first eV) and the *dI/dE* values (the resonances disappear). As illustrated in Fig. 5, taking *ΔE*=1 eV is sufficient to include the bound states and therefore reproduce the resonances and complete the bands. The additional states introduced by taking higher values of *ΔE* only improve the completeness of the basis and serve essentially to remove unphysical discontinuities in the bands.

The relation between resonances in the transmission currents and quasi-bound states in the system was well described by Price [13-15], who actually relates them to poles of the *S* matrix (whose elements are considered as functions of the energy). The present simulations show that these effects are addressed properly, provided additional basis states are considered in the intermediate Region II (through *ΔE*>0). The "interior states" do not need to be computed explicitly, nor treated differently from "open states" [9-10]. The specificity of our approach is to use non-square transfer matrices [17] to prevent instabilities when making the connection between the different regions.

4. Conclusions

This paper was a pedagogical presentation of the transfer-matrix technique, with an extension to extract the band structure of periodic materials from the *T* matrices associated with a single unit. Because of the transfer-matrix formulation of the scattering problem, the band structure is projected on the k_z axis, which is often appropriate in situations where this technique can be applied.

We provided calculations of the transmission and band structure of electrons confined in a cylindrical wire and subject to cosine potentials. We observed how fast the transmission diagram exhibits characteristics predicted by the band structure (namely gaps and steps associated with the opening of new bands), while keeping features associated with their finite length. Comparisons could be made with results obtained for a semiconducting (10,0) carbon nanotube, confirming and providing an insight on processes observed in complex structures.

The issue of bound states was considered. Although they exist only in the intermediate region, they need to be included in the representation because of their impact on propagative solutions (as localized resonances in the transmission) and to avoid unphysical truncations of the bands. Considering additional states essentially improves the completeness of the representation and solves for discontinuities in the bands. The connection between the intermediate region (which may contain "interior states") and the neighboring ones (which contain only propagative states) is achieved using non-square transfer matrices, making the technique perfectly stable.

Acknowledgments

A.M. is supported as Research Associate by the National Fund for Scientific Research (FNRS) of Belgium. The author acknowledges the use of the Namur Scientific Computing Facility and the Belgian State Interuniversity Research Program on *Quantum size effects in nanostructured materials* (PAI/IUAP P5/01). We acknowledge P.H. Cutler, N.M. Miskovsky and Ph. Lambin for useful discussions.

References

[1] J. B. Pendry, J. Mod. Opt., 41 (1994) 209-29.
[2] J. B. Pendry, A. MacKinnon, Phys. Rev. Lett., 69 (1992) 2272.
[3] J. B. Pendry, J. Phys. Condens. Matt., 8 (1996) 1085-1108.
[4] J. B. Pendry, A. MacKinnon, Phys. Rev. Lett., 69 (1992) 2772-5.
[5] J.-P. Vigneron, I. Derycke, T. Laloyaux, P. Lambin, A. A. Lucas, Scanning Microscopy Supplement, 7 (1993) 261-68.
[6] W. D. Sheng, J. B. Xia, J. Phys. Condens Matt., 8 (1994) 3635-45.
[7] P. St. J. Russel, T. A. Birks, F. D. Lloyds-Lucas,
"Confined Electrons and Photons", New York (1995).
[8] A. J. Ward, J. B. Pendry, J. Mod. Opt., 44 (1997) 1703-14.
[9] B. F. Bayman, C. J. Mehoke, Am. J. Phys., 51 (1983) 875-83.
[10] H. Wu, D. L. Sprung, Appl. Phys. A, 58 (1994) 581-7.
[11] M. C. Yalabik, IEEE Trans. Electron Dev., 41 (1994) 1843.
[12] E. Anemogiannis, E. N. Glytsis, T. K. Gaylord, Superlattices Microstruct., 22 (1997) 481-96.
[13] P. J. Price, Superlattices Microstruct., 20 (1996) 253-60.
[14] P. J. Price, J. Appl. Phys., 79 (1996) 7381-2.
[15] P. J. Price, Microelectroncs Journal, 30 (1999) 925-34.
[16] A. Mayer, J.-P. Vigneron, Phys. Rev. E, 59 (1999) 4659-66.
[17] A. Mayer, J.-P. Vigneron, Phys. Rev. E, 61 (2000) 5953-60.
[18] A. Mayer, J.-P. Vigneron, Phys. Rev. E, 60 (1999) 7533-40.
[19] V. T. Binh, V. Semet, N. Garcia, Ultramicroscopy, 58 (1995) 307-17.
[20] A. Mayer, J.-P. Vigneron, Phys. Rev. B, 56 (1997) 12599-607.
[21] A. Mayer, J.-P. Vigneron, J. Phys. Condens. Matt., 10 (1998) 869-81.
[22] A. Mayer, J.-P. Vigneron, Phys. Rev. B, 60 (1999) 2875-82.
[23] A. Mayer, J.-P. Vigneron, Phys. Rev. B, 62 (2000) 16138-45.
[24] A. Mayer, J.-P. Vigneron, Phys. Rev. B, 65 (2002) 195416.
[25] A. Mayer, N. M. Miskovsky, P. H. Cutler, J. Vac. Sci. Technol. B, 20 (2002) 100-4.
[26] M. Abramowitz, I.A. Stegun, "Handbook of Mathematical Functions", New York (1972).
[27] Indeed a reference potential of $-\Delta E$ is assumed between adjacent layers to maintain stability, so the calculations within [0,D] only involve square transfer matrices. It is only when connecting the solutions with those in Regions I and III, where the reference potential is zero that non-square transfer matrices are needed.